LLNL-ABS-766222

v. 9g   January 31, 2019

OSA / Fourier Transform Spectroscopy, San Jose CA, June 25-27, 2019

A 1000x Stabler Spectrograph using an Interferometer with Crossfaded Delays

David J. Erskine
Lawrence Livermore Nat. Lab., 7000 East Ave, Livermore, CA 94550
erskine1@llnl.gov

Eric V. Linder
Berkeley Center for Cosmological Physics & Berkeley Lab, University of California, Berkeley, CA 94720, USA

Abstract: We describe a data analysis strategy weighting signal components from at least two overlapping delays in an externally dispersed interferometer that reduces by 1000x the net shift in response to a wavelength drift in the disperser.

OCIS codes: (300.632) Spectroscopy, High Resolution, (120.2650) Fringe analysis, (120.3180) Interferometry

1. Introduction

Modern astrophysics has demands for extremely stable wavelength measurements, such as 10 cm/s scale Doppler radial velocimetry for earth-like planet detection [1], and cosmic redshift drift measurements [2]. The chief instrumental challenge is not spectral resolution in resolving the feature, but wavelength stability: the point spread function (PSF) of conventional spectrographs drifts in position and shape under duress from thermal changes to the diffraction grating, fluctuations of air internal and external to spectrograph, a changing pupil as target moves across the sky, and flexure of optical fibers (creating mode changes in profile) if fibers are used to communicate the light. Conventional means for mitigating PSF drift include thermal control, vacuum tanks, adaptive optics, fiber optic scramblers, and laser frequency comb calibrants. These measures reduce the “insult”, $\delta\lambda_{insult}$, which reduces the error in the final spectrum. For purely dispersive spectrographs, $\delta\lambda_{final} = \delta\lambda_{insult}$, since the spatial scale of the detector is directly linked to the final spectrum.

While we recommend use of these mitigations if affordable, we propose that dispersive spectrograph stability can be further improved by 2 or 3 orders of magnitude by inclusion of a Michelson interferometer in series, as in externally dispersed interferometry (EDI) [3–7]. In this method the detailed wavelength determination is mostly decoupled from the spatial scale in the disperser and its drift $\delta\lambda_{insult}$. Instead, the detailed wavelength is determined by the phase of a fringe (intensity measurement) in an interferometer cavity, which is calibrated by a spectral reference such as an iodine cell, ThAr lamp or aforementioned laser frequency comb. The cavity PSF is sinusoidal and has only three degrees of freedom (amplitude, period, phase). This is much easier to control or calibrate than the hundreds of degrees of freedom for a disperser PSF (at least one per grating groove).

Hence now the final PSF drift is given by $\delta\lambda_{final} = \delta\lambda_{insult} * TRC$, where TRC is the translation reaction coefficient of the spectroscopic method used. For dispersive spectroscopy TRC = 1; but for EDI using multiple delays we show (Sect. 10 of Ref. 6) how to theoretically make TRC = 0. In recent demonstrations on a single ThAr line using the same data analysis software used in the project, we have obtained TRC as small as 1/1000, which is very exciting. In our previous work we showed that the benefit of multiple delays, but without special weights, can achieve TRC ∼1/20 [6]. In recent work however we used a technique called “crossfading” using strategically chosen weightings to force phase cancellation between a pair of delays, and now have improved stability to TRC ∼1/1000 (Fig. 1).

The crossfading technique works because under the same detector wavelength drift, EDI signals measured by a high delay twist in one direction, and by a low delay twist in the opposite direction. For final spectrum frequencies that lie in between a pair of delays (that overlap), we choose weightings that cancel the net phase shift. We do this for every pair of delays for each frequency, up to a limiting frequency of the highest delay. (We have higher delays which cannot be used for crossfading because they do not overlap sufficiently).

The caveat is that both delays of a pair need to suffer the same $\delta\lambda_{insult}$. Hence we propose modifying the interferometer (as in Fig. 45 of Ref. 6) to measure at least two delays simultaneously, so that all time scale drifts (i.e. including air convection) are defeated. Otherwise, only the drifts longer than the time scale of sequential delay data exposures are mitigated. Crossfading also works with a single delay that overlaps the native PSF, and this stabilizes against drifts of all time scales. We have verified that crossfading also stabilizes against changes in PSF width or asymmetry.

In summary, we propose use of a crossfading EDI alongside of conventional mitigations, because spatial drift of the disperser PSF is a dominant error source for current radial velocity spectrographs, and the stability benefits multiply. If using a fiber scrambler or vacuum tank provides, say, a 10^4 PSF drift reduction, then including the EDI could produce a 10^4*1000 = 10^7 net reduction. Prepared by LLNL under Contract DE-AC52-07NA27344.

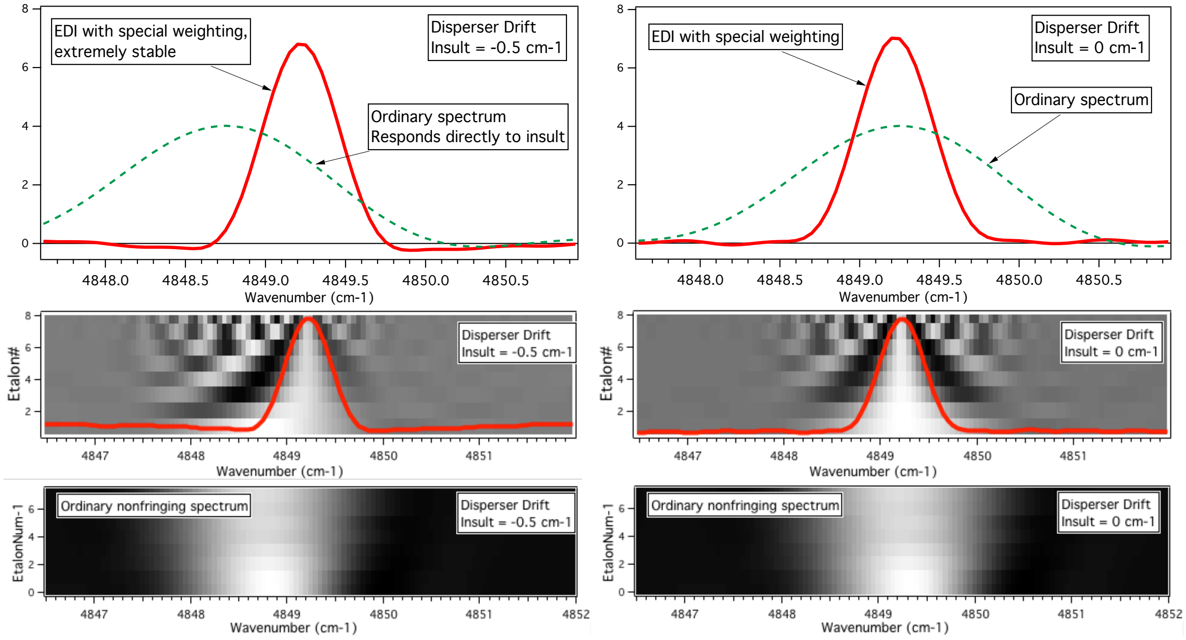

Fig. 1. A multiple delay externally dispersed interferometer boosts the stability and resolution of the disperser in series with it. Precision wavelength is obtained from the interferometric fringe phase, not the disperser, which mainly affects the fringe envelope (middle panels). Multiple delays (etalons) are used having different periodicities, which are summed to form the net EDI peak (red curve). Mt. Palomar Obs. measured [6] ThAr lamp line data (right panels) is artificially shifted on the detector by 0.5 cm^{-1} (left panels). The disperser peak (green dashes) shifts directly, while the net EDI peak moves only $1/1000^{th}$ the amount.

References

1. D. A. Fischer, G. Anglada-Escude, P. Arriagada *et al.*, "State of the Field: Extreme Precision Radial Velocities," Proc. Astr. Soc. Pacific **128**, 066,001 (2016).
2. A. G. Kim, E. V. Linder, J. Edelstein, and D. Erskine, "Giving cosmic redshift drift a whirl," Astroparticle Physics **62**, 195–205 (2015).
3. D. J. Erskine, "An Externally Dispersed Interferometer Prototype for Sensitive Radial Velocimetry: Theory and Demonstration on Sunlight," PASP **115**, 255–269 (2003).
4. J. Ge, J. van Eyken, S. Mahadevan, C. DeWitt, S. R. Kane, R. Cohen, A. Vanden Heuvel, S. W. Fleming, P. Guo, G. W. Henry, D. P. Schneider, L. W. Ramsey, R. A. Wittenmyer, M. Endl, W. D. Cochran, E. B. Ford, E. L. Martín, G. Israelian, J. Valenti, and D. Montes, "The first extrasolar planet discovered with a new-generation high-throughput Doppler instrument," ApJ **648**, 683–695 (2006).
5. P. S. Muirhead, J. Edelstein, D. J. Erskine, J. T. Wright, M. W. Muterspaugh, K. R. Covey, E. H. Wishnow, K. Hamren, P. Andelson, D. Kimber, T. Mercer, S. P. Halverson, A. Vanderburg, D. Mondo, A. Czeszumska, and J. P. Lloyd, "Precise Stellar Radial Velocities of an M Dwarf with a Michelson Interferometer and a Medium-Resolution Near-Infrared Spectrograph," PASP **123**, 709 (2011).
6. D. J. Erskine, J. Edelstein, E. H. Wishnow, M. Sirk, P. S. Muirhead, M. W. Muterspaugh, J. P. Lloyd, Y. Ishikawa, E. A. McDonald, W. V. Shourt, and A. M. Vanderburg, "High-resolution broadband spectroscopy using externally dispersed interferometry at the Hale telescope: part 1, data analysis and results," Journal of Astronomical Telescopes, Instruments, and Systems **2**, 025004 (2016).
7. D. J. Erskine, J. Edelstein, E. Wishnow, M. Sirk, P. S. Muirhead, M. W. Muterspaugh, and J. P. Lloyd, "High-resolution broadband spectroscopy using externally dispersed interferometry at the Hale telescope: part 2, photon noise theory," Journal of Astronomical Telescopes, Instruments, and Systems **2**, 045001 (2016).